THE ASTROPHYSICAL JOURNAL, Vol. 151, March 1968

NORMAL OH EMISSION AND INTERSTELLAR DUST CLOUDS

CARL E. HEILES
Berkeley Astronomy Department, University of California

Received August 23, 1967; revised September 21, 1967; and in proofs

ABSTRACT

Normal emission from OH in interstellar dust clouds has been detected. The clouds have normal cosmic abundances; the hydrogen, which is not observed to emit 21-cm line radiation, is probably all H_2. The amounts of OH and H_2 are consistent with statistical equilibrium with known reactions. The clouds are sufficiently opaque to exclude nearly all of the galactic radiation field so that photodissociation does not occur; also, the resulting radiation pressure differential helps hold the clouds together.

I. INTRODUCTION

Normal OH radio line emission from spatially extended regions has heretofore never been detected. This paper reports the detection of such emission from very dark dust clouds and analyzes the properties and physical processes characterizing these objects.

Previously known OH emission is abnormal: the line ratios are abnormal, the emission is polarized, the sources are very small, and the emission is sometimes time-variable. OH has also been detected in absorption; these data indicate that it is sometimes distributed throughout the interstellar medium and sometimes concentrated around H II regions and often shows abnormal line ratios. For observations and references to previous literature the reader is referred to the recent papers by Palmer and Zuckerman (1967), Weaver, Dieter, and Williams (1968), and Goss (1967).

II. EQUIPMENT AND PROCEDURE

The 85-foot telescope and 100-channel filter receiver of the Hat Creek Radio Observatory used for these observations will be described by Weaver *et al.* (1968). The system temperature was typically 150° K throughout the observing periods. Channels of width 2 kHz were used, so that the total band width examined was 200 kHz.

The initial search was performed during a few days in February and March, 1967; during this time the 1667 MHz line radiation was detected and the 1720 MHz line was attempted. In June and July, 1967, the objects were mapped and measurements of all four lines were made at some positions.

The observational procedure differs somewhat from that used in the past at this observatory and because it yields an increase in useful telescope time we describe it in detail. The output O, in millivolts, of an individual channel is given by

$$O = G[T_a^f - \tfrac{1}{2}(T_a^{f+w} + T_a^{f-w})] + G[T_r^f - \tfrac{1}{2}(T_r^{f+w} + T_r^{f-w})] + Z , \qquad (1)$$

where G is the channel's gain and Z its zero shift; T_r and T_a are the receiver noise and antenna temperatures, respectively; the superscript f denotes the observing frequency, and w denotes the difference between the observing frequency and the comparison frequencies. The first term on the right-hand side is the quantity of interest. The last two represent instrumental base-line shifts and must be eliminated by measuring them separately. It has been found that Z is independent of the noise power entering the filter; the present procedure hinges on this point.

In the past the Z's were established by observing a comparison region in which no OH is present. Because the result of this observation was uncertain due to receiver noise, it was necessary to spend as much time observing the comparison region as the source.

But Z can be established by disconnecting the front end, since Z is independent of the noise power entering the channel; in this case the uncertainty due to receiver noise disappears, and much less time is necessary to make the measurement.

The above procedure establishes the individual channel zero shifts, but does not establish the base-line shift due to variation of T_r with frequency. This variation is broad band, since it is due to the band pass of the front end; it can be extremely well approximated by a straight line for the present observations because the total band width examined, 200 kHz, is much smaller than the front-end band pass. The two parameters of this straight line were determined by a least-squares fit to the values $(O - Z)$ of all 100 channels obtained in an observation of a comparison region.

It is not necessary to spend equal time on the comparison region, however, because the two parameters of the straight line are determined from 100 independent numbers so that their uncertainty is about $\frac{1}{10}$ the uncertainty of an individual channel. We considered an uncertainty in base-line slope equal to $\frac{1}{3}$ the uncertainty in an individual channel, for an observation of the source, to be acceptable since we were expecting narrow lines. Thus the individual channel uncertainty for the comparison region could be about three times that for the source, so that the comparison region need be observed only 10 per cent of the time, rather than 50 per cent as with the previous method.

A least-squares straight line fit to the base line was subtracted from the profiles presented herein to remove the residual slope resulting from this observation procedure; in no case did we suspect this slope to be real. (Only the 1667 MHz profile for cloud 2 [see Fig. 2], obtained during the winter observing period, was reduced the "old" way.)

III. OBSERVATIONS

The dust clouds were selected on two criteria: very large optical absorption; and lack of excess 21-cm line emission from atomic hydrogen. The combination of these two criteria should yield dust clouds in which hydrogen molecules abound (Garzoli and Varsavsky 1966; Heiles 1967*a*, *b*) and we took the naïve viewpoint that if conditions were ripe for formation of H_2 they might also favor the formation of other molecules. (See § IV for quantitative estimates.)

Many outstanding dust clouds exist in the galactic plane; however, some of these clouds appear outstanding because the star density is high in the Milky Way. The situation at intermediate galactic latitudes is somewhat different because the star density is quite low; here for a dark cloud to be outstandingly obvious it must be nearby, fairly large, and very dark. Of prime importance is the narrow range of velocity which nearby objects at intermediate latitudes can have. Regions in which Hubble (1934) counted few galaxies at intermediate latitudes were used to locate regions of high absorption; Palomar prints near these regions were used to locate extremely dense, fairly compact dust clouds. Unfortunately 21-cm observations do not exist for most of these regions, so the second criterion could not be applied. For two regions, near cloud 1 and cloud 2, the second criterion could be applied (Garzoli and Varsavsky 1966; Heiles 1967*b*). One object, L134, was chosen from Lynds's (1962) catalogue solely because it could be observed at 11 hours LST when no other objects were above the horizon. Six regions were selected for observation; positions within four yielded positive results. We discuss the properties of these objects below (§ IV*a*); their boundaries, and some of the positions observed, are shown in Figure 1.

The OH Emission

The positions of the comparison regions are given in Table 1. We present the observations yielding negative results in Table 2. We present our OH emission profiles for positive observations in Figure 2, and summarize the properties of the lines in Table 3. All velocities are measured with respect to the local standard of rest defined by van de Hulst, Muller, and Oort (1954). The brightness temperature, T_b, was found from the

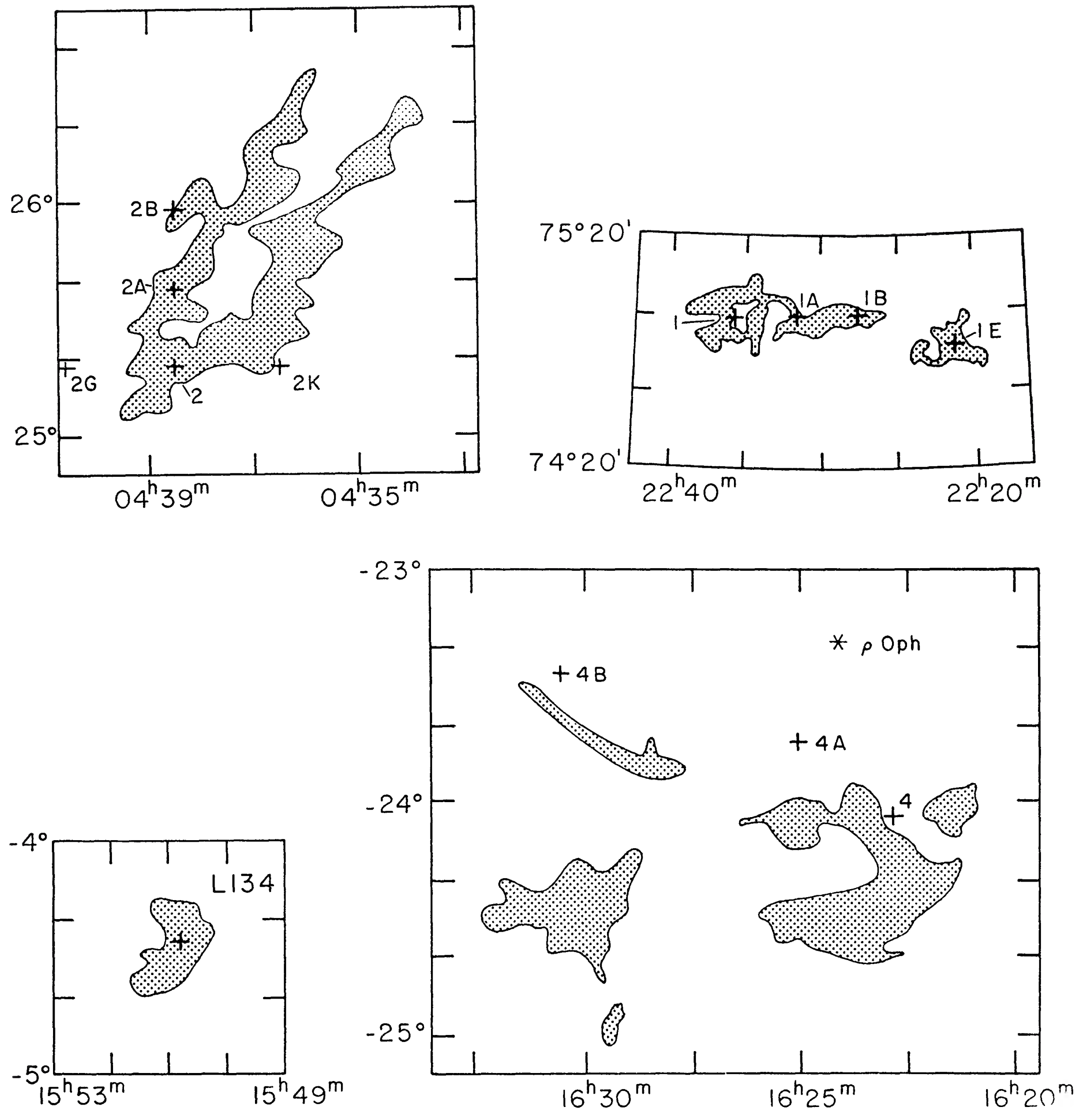

FIG. 1.—Sketches showing boundaries of the dust clouds studied. The crosses mark some of the position observed; OH emission was not detected from all of these positions (see Tables 2–4).

TABLE 1

COMPARISON REGIONS

Object	α_{1950}	δ_{1950}
Cloud 1-1F .	$22^h36^m19^s$	77°02′
Cloud 2-2K	04 39 33	27 22
Cloud 4-4E	16 55 14	−24 03
Cloud L134	15 36 45	−04 26 5

TABLE 2

OBSERVATIONS YIELDING NEGATIVE RESULTS

Object	α_{1950}	δ_{1950}	Line	Peak-to-Peak Noise (° K)
1A ..	$22^h31^m55^s$	+74°58′	1720	0 25
1A .	22 31 55	+74 58	1612	25
1E	22 21 30	+74 51	1667	.3
1F ..	22 14 45	+73 07	1667	.3
2	04 38 30	+25 18	1720	3
2.	04 38 30	+25 18	1612	3
2E	04 38 30	+24 38	1667	5
4	16 24 15	−24 04	1720	3
4 .	16 24 15	−24 04	1612	3
4A* ..	16 26 00	−23 45	1667	3
4B* . .	16 30 25	−23 27	1667	.4
4C* ..	16 36 30	−23 49	1667	4
4E*.	16 42 40	−21 16	1667	35
5	16 44 44	−11 55	1667	3
5A	16 44 44	−12 15	1667	0 3

* Dust cloud not in beam—see text.

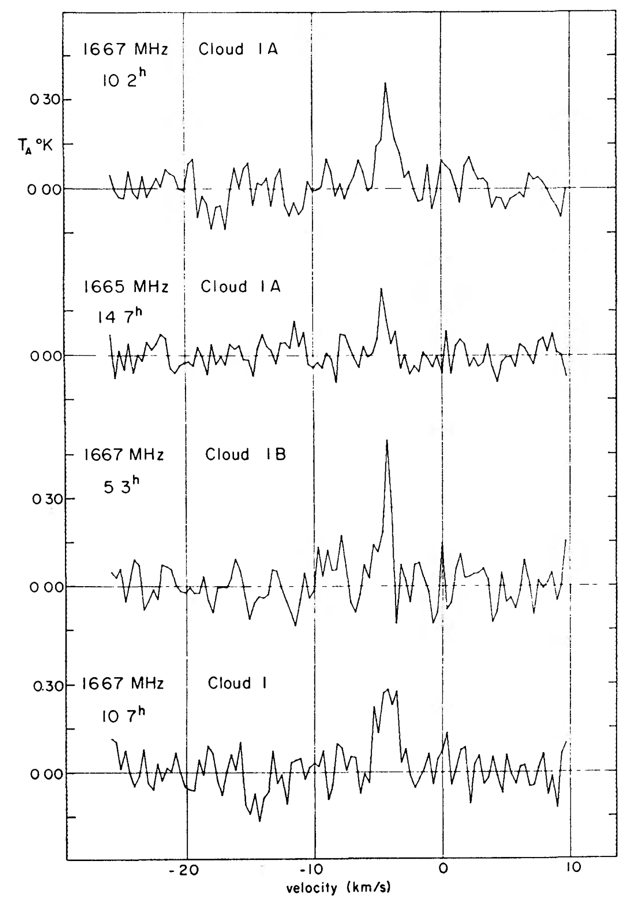

FIG. 2.—Profiles of antenna temperature versus velocity (with respect to LSR) which yielded positive results. The integration time in hours is indicated for each profile. See Table 3.

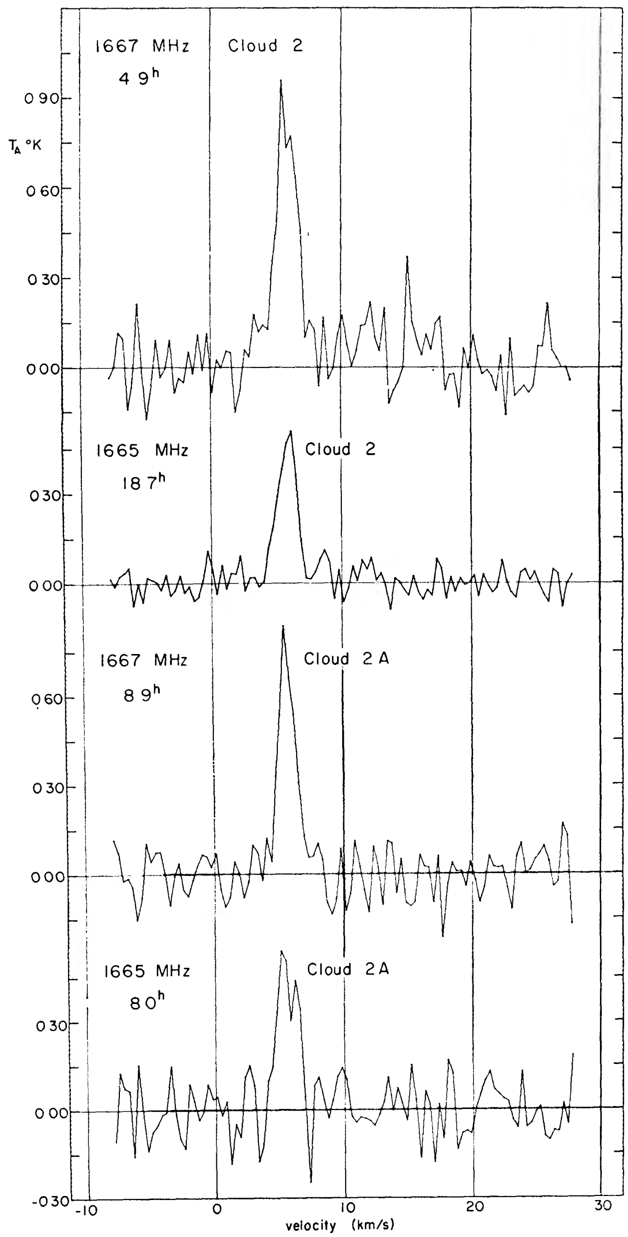

FIG. 2—*Continued*

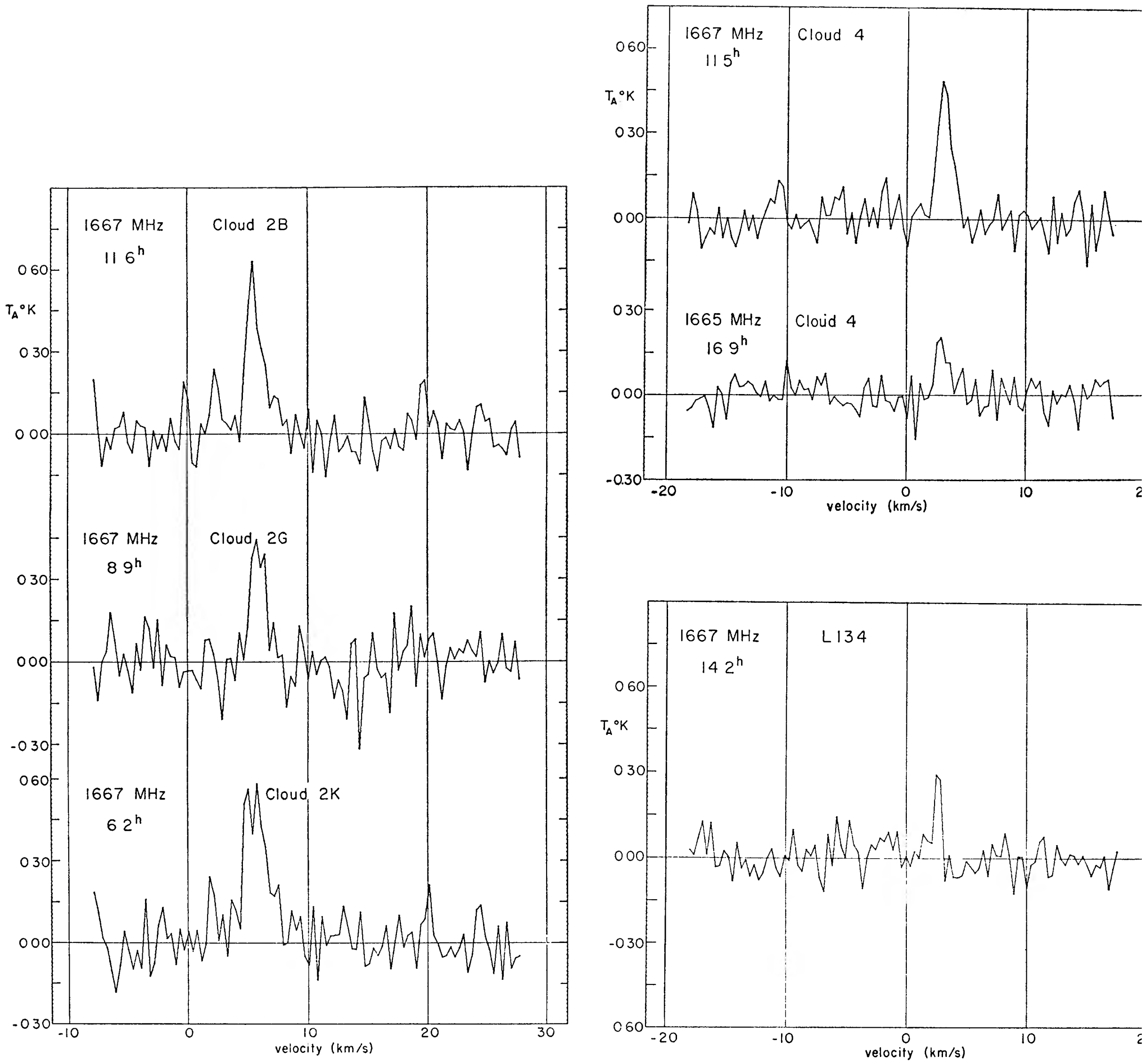

FIG. 2—*Continued*

TABLE 3

PROPERTIES OF OH EMISSION

OBJ.	α_{1950}	δ_{1950}	LINE (MHz)	GAUSSIAN PARAMETERS			DILUTION FACTOR	N_{OH}	n_{OH} ($\times 10^{+6}$)	T_s	
				T_a max	Full Half-Width (kHz)	Velocity (km/sec)				Lower	Upper
1	22^{h}35^{m}55^s	74°58′	1667	0.290	10 03	−4.02	0 143	3 6±2.4×10^{13}	4.0	. .	340
1A.	22 31 55	74 58	1665	.178	5.11	−4.22	.120	2.9±3 1×10^{13}	4.5	*	230
A.	22 31 55	74 58	1667	.280	8.73	−3.87	.120	5.2±3.1×10^{13}			
1B	22 27 55	74 58	1667	472	4.03	−4.01	137	3 6±2.7×10^{13}	4.0	. .	140
2	04 38 30	25 18	1665	494	9.82	+6.12	.294	6.9±1.3×10^{13}	1.5	6.5	350
2.	04 38 30	25 18	1667	.829	11.88	+6.12	.294	7 6±1.6×10^{13}			
2A.	04 38 30	25 38	1665	.519	9 79	+5 78	.296	6.8±2.5×10^{13}	1.4	5.6	310
2A.	04 38 30	25 38	1667	758	8.86	+5.90	.296	6.8±1.3×10^{13}			
2B	04 38 30	25 58	1667	499	10 04	+5.90	.198	6.6±2.1×10^{13}	1.4	. .	340
2G.	04 40 30	25 18	1667	432	8.40	+6.24	064	1.9±0 6×10^{14}	4.0	. .	280
2K.	04 36 30	25 18	1667	.509	13.54	+5.91	.245	6.6±1.7×10^{13}	1.4	. .	460
4.	16 24 15	−24 04	1665	.179	7.87	+3 62	.272	3 4±1.5×10^{13}	0.95	5 6	260
4.	16 24 15	−24 04	1667	467	7.86	+3 69	.272	3.2±1.2×10^{13}			
L134.	15 50 50	−04 26	1667	0.348	3.22	+3 02	0 171	1.7±0.8×10^{13}	0.57	. .	96

* Not computed due to large uncertainty in N_{OH}.

antenna temperature by assuming the OH emission to come from the area pictured in Figure 1 with uniform brightness; to obtain the dilution factor the area was smeared with the beam of the antenna, for which we approximated the directive gain, D, as

$$D = \frac{0.8}{\pi \sigma^2} \exp - \left(\frac{\theta}{\sigma}\right)^2 \tag{2}$$

with $\sigma = 20'$ arc. The factor 0.8 represents the beam efficiency and is uncertain by about 10 per cent (W. J. Welch, private communication). The projected density of OH was computed from the integral of brightness temperature over frequency according to the standard relations using the transition probabilities given by Turner (1966) and assuming a negligible optical depth. These integrals were computed by summing the brightness temperatures of the channels centered on the line over a range of about three times the line width, and subtracting the average of similar sums taken on each side of the line. The quoted errors were obtained by multiplying the peak-to-peak noise on the profile by the square root of the number of channels used in the sum and the channel width (2 kHz). We consider the integrals derived in this way more reliable than those obtained from a Gaussian fit (see below). For all objects the projected density so obtained from the 1665 and 1667 MHz lines is the same, within the experimental error; since in no case were the satellite lines detected, we conclude that the line ratios appear normal and that the optical depth is in fact small.

Our observational limits on the optical depth are of interest because they yield lower limits on the spin temperature T_s via the solution of the equation of transfer for a uniform cloud,

$$T_b = (T_s - 3^\circ)(1 - e^{-\tau}) . \tag{3}$$

The 3° represents the contribution of the cosmic microwave background (see Goss [1967] for a complete discussion of the equation of transfer for OH). The brightness temperature at the peak of the profile yields the largest lower limit; it was obtained by fitting the profiles with a Gaussian curve according to the least-squares method using a computer program developed by N. Dieter and A. Ebert. The lower limit for T_s in Table 3 is the smallest consistent with the error in the peak of the Gaussian curve. Note our lower limits are larger than the spin temperatures obtained in previous work for OH in other circumstances (see Goss 1967).

The half-width of the Gaussian reflects the turbulent, thermal, and systematic velocity field within the cloud and thus yields an upper limit to the kinetic temperature. The kinetic temperature cannot be smaller than the spin temperature if T_s is determined by collisional processes, as envisioned below (§ IV*e*); thus this limit probably also applies to the spin temperature. These two limits, given in Table 3, bound the spin temperature. However, we regard the general procedure of least-squares fitting of a Gaussian function to an OH profile as highly artificial because there is no a priori reason why the turbulent and systematic velocity fields should be of this form. The velocity dispersion obtained from this procedure may bear little relation to the actual value of kinetic temperature and is used only in the absence of accurate data.

IV. INTERPRETATION

a) *The Dust Clouds*

The objects together with many of their properties are listed in Table 4. Their boundaries were obtained by casual inspection of the red Palomar prints. The dust clouds appear somewhat larger on the blue prints; use of the red prints underestimates the total extinctions and projected dust densities derived below. It will be noted that the observed positions for cloud 4 do not fall within the dust cloud but instead lie systematically north; this was a blunder on the part of the author.

The total extinction of each cloud was estimated by measuring its apparent area and counting the number of stars visible within it; this yields the number of stars per square degree within the cloud brighter than the magnitude limit of the red Palomar prints, taken as 20. This quantity was compared with the average number of stars per square degree brighter than magnitude m given by van Rhijn (1929) near the galactic latitude of the cloud. Let the magnitude for which these two quantities are equal be m'. Then stars which would be dimmer than m' in the absence of the dust cloud are made invisible because the dust has made them dimmer than the Palomar print limit. If the cloud is in front of all the stars in the field, the extinction of the dust is simply $(20 - m')$ mag; if not, it is even greater. The total extinctions listed in Table 4 were derived under this assumption. Their values, typically 8 mag, are very high; such high extinctions for these regions have never been reported in previous literature to this author's knowledge.

TABLE 4

PROPERTIES OF DUST CLOUDS

	OBJECTS				
	1–1D	1F	2	4	L134
l^{II}	114 5	111 8	174 6	353 4	4 2
b^{II}. ...	14 6	14 0	− 13 7	16 9	35 8
Area (sq degree).	0 086	0 016	0 49	0 53	0 079
No. stars within . .	3	2	26	17	0
Total excitation (mag) lower limit	8 0	6 5	8 0	8 0	8 5
Distance (pc) .	500	400	113	77	170
Source for distance	Heiles (1967*a*); Slocum and Sitterly (1937)	HD 210806	McCuskey (1941)	ρ Oph	*
Radius (pc).... . .	1 5	0 5	7 8	0 55	4 7
Density of dust (grains/ cm^3)	1 5×10^{-10}	3 5×10^{-10}	2 8×10^{-11}	3 8×10^{-10}	4 8×10^{-11}
H_2 density (molecules/ cm^3)	220	510	42	570	73
Total mass ($M_\odot$).. .	220	22	6400	1900	2500
β†.... . ..	0 080	0 046†	0 24	0 023	0 58
$\beta_{(r)}$...	0 085	0 074†	0 26	0 025	0 54

* Height above galactic plane assumed = 100 pc.
† Assuming $T_K = 100°$ K.

It is instructive to compare our total extinctions with those available in the literature. McCuskey (1941) states that the densest part of the Taurus dark nebula absorbs 4.90 mag (pg) over an area of 3.5 sq. degrees. By casual inspection of the Palomar prints it is obvious that the area of cloud 2 is much less than 3.5 sq. degrees; thus he has probably underestimated the total extinction within the very darkest parts of the 3.5 sq. degree area. The difference between his results and ours probably results from the limiting magnitude of his plates, only 15 or 16 (Miller 1938). Müller (1931) derives a total extinction of 2.8 mag (pg) for cloud 4 near the star ρ Oph; however, he considered a large area (15.7 sq. degrees) and also used plates of limiting magnitude 15. The total extinction in front of the binary ρ Oph can be calculated from the distances, apparent visual magnitudes, and spectral types given by Hoffleit (1964) and from the absolute visual magnitudes given by Keenan (1963). The average total extinction of the two components is 3.7 mag (visual). But ρ Oph lies outside of the boundaries of cloud 4 (see Fig. 1) so that this value is certainly a lower limit for the extinction in cloud 4.

Even the Palomar prints are inadequate for obtaining total extinctions from star counts because too few stars are visible within the dust clouds. Because our method gives the correct result only if the cloud is in front of all the stars in the field, we consider the estimates in Table 4 to be *lower limits*—even though the total extinctions seem extreme. We apologize for our crude estimates of the properties of these dust clouds; significant improvement in accuracy is possible only if a detailed study is undertaken.

The distance to a cloud is obtained from estimates by other workers which refer either to our specific cloud or to a nearby one; or from the distance to a star which seems to be illuminating nearby dust as a reflection nebula. These sources of information are listed in Table 4. Bok's (1937) criticism of deriving distances directly from Wolf diagrams was kept in mind, particularly for Müller's (1931) distance estimate for cloud 4.

The size of a cloud is an ill-defined quantity because of its typically irregular shape. However, some characteristic size must be adopted for an estimation of its extent in the line of sight so that the projected density can be converted to a volume density. The radius of a cloud was taken as

$$r = (\text{area}/\pi)^{1/2} . \tag{4}$$

The projected density of dust was computed from the total extinction using the formulae given by Lilley (1955), assuming all dust grains have radii $= 3 \times 10^{-5}$ cm. The volume density was obtained by dividing the projected density by $2r$, and the total mass of dust was obtained by multiplying that volume density by $4\pi r^3/3$.

The total mass, including material other than dust grains, was obtained by dividing the mass of dust by 0.014. This is the cosmic abundance by mass of heavy elements other than helium (Allen 1963); if the chemical abundance in a cloud is normal and the grains consist mainly of heavy elements other than helium, our total mass is a lower limit because some heavy elements may not be tied up in the grains. (It is also a lower limit because the total extinction given in Table 4 is itself a lower limit.) We justify this procedure in more detail in § IV*b*. Given the total mass and size of an object we can compute the ratio β = (gravitational potential energy)/(twice kinetic energy), equal to one if the object is in equilibrium (see Heiles 1967*b*); the velocity dispersion used was derived by a least squares Gaussian fit to the profiles, which underestimates β if large scale motions contribute to the observed dispersion (Heiles 1967*c*).

It is presumed that little or no excess 21-cm line radiation is emitted from these clouds; this fact is known for cloud 2 (Garzoli and Varsavsky 1966). Thus the hydrogen must all be molecular; the number density of H_2 computed from the total mass of the object, accounting for the presence of helium, is also given in Table 4 (for adopted abundances see Allen 1963).

We present detailed evidence supporting this presumption for another case. In Figure 3 (Plates 8 and 9) we reproduce Heiles' (1966) 21-cm line data for constant-declination scans passing through clouds 1–1E and 1F. The scan shown in Figure 3*a* passes through clouds showing OH emission; the observed positions and OH velocities are denoted by crosses. The OH velocity lies in between the velocities of the hydrogen sheets; perhaps this dust cloud is being compressed if the sheets are approaching (see Heiles 1967*b*). The position of cloud 1F, from which OH emission was *not* detected, is shown in Figure 3*b;* some excess 21-cm emission does appear near velocity -1 km/sec, corresponding to a projected density of about 10^{19} hydrogen atoms/cm^2 (volume density $\simeq 5$ atoms/cm^3; see Table 4). This projected density is far less than that expected from the data given in Table 4, indicating that only about $\frac{1}{50}$ of the hydrogen has escaped conversion to H_2. We now discuss the significance of this data in detail. It is unfortunate that detailed 21-cm line data are unavailable for the other objects.

b) The Chemical Abundances in the Clouds

It is necessary to consider the possibility that a dust cloud is bound by the pressure of the interstellar radiation field (Whipple 1946) and that the gas within the cloud has diffused away. This process would lead to the separation of gas atoms from the dust grains—and thus to a large excess of heavy elements within the cloud. The radiation pressure, p_r, is probably about 5.2×10^{-13} dynes/cm^2 (Dunham 1938); its effect on the stability of each cloud is given in Table 1 where β_r, the ratio equivalent to β for gravitational stability, is given by

$$\beta_r = \frac{p_r}{p_i} = \frac{3770}{nT}. \tag{5}$$

Here p_i is the pressure inside the cloud due to gas atoms, and we assume zero radiation density inside the cloud. The numerical values were computed for a temperature equal to the upper limit for T_s given in Table 3. Their values indicate that radiation pressure is not unimportant in holding the clouds together.

The radiation pressure acts directly only on the grains and if self-gravity is unimportant the gas will expand, leaving the dust behind. The time scale for this is of order r/v, where r is the cloud radius and v is the thermal velocity of the gas atoms; this assumes zero external pressure at the boundary of the cloud (Heiles 1967*c*). For $v = 10^5$ cm/sec this time ranges from less than 10^6 years for cloud 1F to about 10^7 years for cloud 2. (Inclusion of atom-grain collisions does not significantly affect these results.) These times seem rather short and are comparable to the times required to establish statistical equilibrium in the reactions described above.

As the gas atoms leave the cloud the interstellar radiation field would rapidly dissociate both the OH (in 10^4 years; Stecher and Williams, 1966) and the H_2 (in 10^3 years; Stecher and Williams 1967); thus objects undergoing this loss will be detectable due to to the 21-cm line radiation of the surrounding H I halo. In this regard the 21-cm line data for cloud 1F is of interest, because excess H I near its position is observed (Fig. 3*b*). These data indicate that the angular half-width of the H I cloud is 29ʹ.8 (after correcting for telescope beam smearing); the angular diameter of the dust cloud is only 15ʹ.6 (in an east–west direction). Thus the excess 21-cm radiation may actually be due to H I lost in the manner envisioned above, especially since the flat-topped angular variation of the H I emission is not inconsistent with a displaced shell source which could result from motion of the dust cloud through the surrounding gas. The object probably is deficient in gaseous constituents hydrogen and helium.

No excess 21-cm radiation is observed near clouds 1–1E. These objects, then, *cannot be losing hydrogen gas* so that the chemical abundances should be cosmic and our mass computation correct. Possible physical explanations for this lack of mass loss are that the cloud density is larger than the lower limit given in Table 4, increasing the value of β; or that T_k is less than the upper limit in Table 3.

c) The Abundance of H_2

H_2 can be formed in significant quantities only by interaction of H I with grains. The mechanism of this interaction is either a chemical exchange reaction or physical absorption (Stecher and Williams 1966).

The chemical exchange reaction rate is much too slow at the low temperatures given in Table 4 to produce H_2 in the required quantity. We could speculate that our dust clouds were all subject to shock waves which raised their temperatures to several thousand degrees; the reaction rate at 3000° K is about 10^8 the rate of 100° K. However, the material behind the shock cools very rapidly, in a few thousand years (Field, Rather, Aannestad, and Orszag 1968), and again insufficient time is available to form the required amount of H_2.

The process of physical adsorption occurs only if the grain temperature is less than 4.5 to 7.5° K (Knapp, van den Meijdenberg, Beenakker, and van de Hulst 1966); otherwise an adsorbed hydrogen atom will escape before another is adsorbed. The temperature of dust grains in interstellar space is typically 15° K (van de Hulst 1949); it results from an equilibrium between heating by the interstellar radiation field and cooling by thermal radiation from the grain. Since in very dark clouds the interstellar radiation field is dimmed the heating rate will be smaller, and the grains cooler, than in typical interstellar regions.

The optical depth in red light, 6500 Å, through a typical cloud is about 8 mag; the optical depth to the center of the cloud is half this. The optical depth in the ultraviolet, where most of the energy density of the radiation field lies, is larger by a factor of about 2.4 because of reddening (Swamy and O'Dell 1967); this value is rather uncertain because it depends on how the reddening curve is extrapolated to zero wavelength. Thus the optical depth to the center of the cloud in the ultraviolet is about 9.6 mag. The heating rate is thus decreased by a factor exp $(-\tau) \cong \frac{1}{7000}$. The cooling rate of a grain is proportional to the fifth power of its temperature (see Wickramasinghe 1965); thus the equilibrium temperature of our grains will be $7000^{1/5} \cong 6$ times smaller than the 15° K of grains in typical interstellar space. The resulting temperature, 2.5° K, is certainly small enough to prevent adsorbed hydrogen atoms from escaping from grains too rapidly. (Grain heating due to collisions with H_2 at $T_k = 100°$ K occurs at about $\frac{1}{3}$ the rate of heating by radiation obtained here.) This temperature is so low, in fact, that the hydrogen molecules may not be able to escape from the grains so that a monolayer of H_2 would exist (Gould and Salpeter 1963); in this case, too, formation of H_2 by adsorption may not occur. Very large uncertainties exist in our computation of the grain temperature, the most important of which is the uncertainty in the optical depth of the dust clouds; an error of 10 per cent in this quantity yields a factor 10^3 error in the intensity illuminating a dust grain, and thus a factor 4 error in its temperature. We assume the dust grain temperature to be in the range in which the adsorption process occurs.

Under these conditions the rate of formation of H_2 is

$$\frac{dn_{\mathrm{H}_2}}{dt} = \tfrac{1}{8} n_{\mathrm{H}} \bar{v} A \,, \tag{6}$$

where A is the grain surface area per cm^3, and $\bar{v}$ is the mean thermal velocity of the hydrogen atoms (Gould and Salpeter 1963). The time scale for conversion to H_2 is then

$$\tau \cong \frac{8}{\bar{v} A} \text{ sec}. \tag{7}$$

Ths quantity was computed under the assumption $\bar{v} = 10^5$ cm/sec and is on the order of 10^6 years for most of the objects.

The destruction process competing with this formation is excitation to the vibrational continuum by radiation in the 1000 Å region (Stecher and Williams 1967). The dissociation rate per molecule is 5.5×10^{-11} sec^{-1} in normal interstellar regions, but again the absorption of the dust decreases this by $e^{-\tau}$. At 1000 Å the extinction is about 2.9 times that in the red, so that the typical extinction to the center of the cloud is 11.6 mag. The dissociation rate is reduced to 5×10^{-16}, so that its time scale $\cong 7 \times 10^7$ years. The formation rate is much larger than the destruction rate, so essentially all of the hydrogen will be H_2, as was inferred from observational evidence above.

d) The Abundance of OH

We consider two ways of forming OH: the reactions

$$\langle G\rangle \mathrm{H} + \mathrm{O} \rightarrow \langle G\rangle + \mathrm{OH}\,, \tag{8a}$$

and

$$\mathrm{H} + \mathrm{O} \rightarrow \mathrm{OH} \tag{8b}$$

where $\langle G\rangle$ denotes the grain (the reaction $\langle G\rangle O + H \rightarrow \langle G\rangle + OH$ does not occur according to Stecher and Williams 1966; see also Solomon 1968); and the reaction

$$H_2 + O \rightarrow OH + H \tag{9}$$

(Carroll and Salpeter 1966). Of these the latter is predominant in our objects because the H_2 density is so very high (see above), although if H I were detected, reaction (8b) might become a contender. Apparently OH formation by physical adsorption does not occur because the grain instead acquires an ice mantle (Wickramasinghe 1965). We thus adopt reaction (9) as the major one with the following reaction rate, obtained from Stecher and Williams (1966) and Carroll and Salpeter (1966):

$$\frac{dn_{OH}}{dt} = 10^{-12} T^{1/2} e^{-4150/T} \; n_{H_2} n_O \, . \tag{10}$$

We consider four destruction processes for OH: photodissociation; the reaction

$$OH + H \rightarrow O + H_2 \, ; \tag{11}$$

the reaction

$$OH + O \rightarrow O_2 + H \, ; \tag{12}$$

and the reaction

$$OH + H_2 \rightarrow H_2O + H \, . \tag{13}$$

Of these processes rates for the first two were obtained from Stecher and Williams (1966) and for the last two from Carroll and Salpeter (1966). Of these reactions (12) is predominant, mainly because its activation energy is small. The reaction (11) is negligible because, as above, little H I exists in the clouds; reaction (13) is negligible because of the high activation energy; and photodissociation is most rapid, other than reaction (12), but is small because of the large extinction near 1000 Å ($\simeq$11.6 mag; see § IV*b*). The reaction rates are

$$\frac{1}{n_{OH}} \frac{dn_{OH}}{dt} = -10^{-10} n_O e^{-600/T} \tag{14}$$

for reaction (12); and

$$\frac{1}{n_{OH}} \frac{dn_{OH}}{dt} = -3 \times 10^{-12} e^{-\tau} \cong -7 \times 10^{-17} \tag{15}$$

for photodissociation.

The equilibrium abundance foı OH under processes (9) and (12) is

$$n_{OH} = \frac{n_{H_2}}{10} e^{-3550/T} \, . \tag{16}$$

For all objects the temperature required to produce the observed OH abundances is close to 220° K; this is consistent with the limits given in Table 3. The time scale required for establishment of this equilibrium is of the order 10^4 to 10^5 years; and this is much shorter than the time required for complete conversion of H I to H_2. It is extremely doubtful, however, that the temperatures are as high as 220° K (§ IV*e*). Other production processes effective at low temperatures should be investigated; for example, could reaction (9) proceed faster than rate (10) at low temperatures by quantum mechanical tunneling?

Both reactions (9) and (12) require the presence of free oxygen atoms. In computing the reaction rates it has been assumed that none of this oxygen is tied up in the grains—i.e., that the entire supply of oxygen, obtained from the cosmic abundances of Allen (1963), is available as free atomic oxygen. This may not be the case: If grains are made of ice, or if the grains are graphite particles coated by ice, the supply of free oxygen will be diminished.

If the supply of O I is nearly completely depleted, we would have to invoke reactions using no oxygen. Since reactions using H I are not permissible either, we are left with no formation process for OH other than exotic processes such as sputtering of ice grains or mantles (Wickramasinghe 1965) which require a high temperature; we tentatively assume such processes to be inoperative at the present time. The most effective destruction process would be photodissociation, occurring on a time scale of about 10^8 years. Since no formation could occur under present conditions, we would have to invoke OH production in the past when conditions were different; destruction appears sufficiently slow to have left the OH undisturbed. Specifically, these past conditions would have to be: (1) the availability of atomic oxygen, or the availability of atomic hydrogen together with a high temperature (such as in a shock wave; P. A. Aannestad [private communication] has shown that copious OH production occurs under these conditions); and (2) the existence of dust to shield most of the ultraviolet radiation.

e) *Temperatures*

The spin temperature of OH for typical interstellar regions has been calculated in detail by Goss (1967), who finds that for H I densities larger than 50 atoms/cm^3 the OH spin temperature T_s is within a factor 2 of the kinetic temperature T_k for $T_k \cong 100°$ K. His calculations are not directly applicable to our dust clouds because of the heavy extinction which, in particular, shields ionizing radiation so that few ions are expected; these ions are the major contributer to collisional excitation of OH in typical interstellar regions. In our objects the H_2 abundance is extremely high. If we take the OH–H_2 interaction cross-section as the geometrical one, collisions will be about $\frac{1}{4}$ as effective as for the ionic concentrations used by Goss. A crude approximation, then, is to adopt Goss's results directly but increase all his densities by a factor 4; thus the OH T_s is within a factor two of T_k for H_2 densities larger than 100 molecules/cm^3, for example. Reference to the H_2 densities given in Table 4 shows that in only two cases is the H_2 density less than 100 molecules/cm^3, and in those cases Goss's results imply T_s should still be a substantial fraction $(\cong\frac{1}{3})T_k$.

It is difficult to envision how the gas kinetic temperature could be kept very large within the dust clouds because no energy can enter from the outside (except, perhaps, cosmic rays). Cooling, however, is quite efficient at these densities; cooling from H_2-grain collisions alone occurs on a time scale of less than 10^6 years. It would be contrary to present views if the kinetic temperature is in fact as high as permitted by our upper limit, or as required for the OH equilibrium (16). It is unfortunate that our limits on the spin temperature are so poor.

V. SUMMARY AND CONCLUDING REMARKS

Normal emission from OH in interstellar dust clouds has been detected. The amount of OH, typically 10^{-6} molecules/cm^3, is consistent with statistical equilibrium between production by reaction (9) and dissociation by reaction (12) if $T_k \approx 220°$ K; however, no generally accepted heating mechanism could produce such a high temperature and it is more likely that OH is produced more rapidly than equation (10) suggests, perhaps by another process. The dust clouds are very massive and are partially contained by the interstellar radiation field; they may also be gravitationally bound because our mass estimates are lower limits, and the temperatures are probably quite small.

The clouds must have normal chemical abundances, consisting mainly of hydrogen, probably H_2; otherwise the 21-cm line emission of the escaping hydrogen would be observed (as it was for cloud 1F). H_2 has probably been formed by physical adsorption on grains, which can occur because the grain temperature is low inside these objects. The chemical reactions we invoked for H_2 and OH will be effective only inside dense dust clouds where the interstellar radiation field is considerably dimmed; otherwise exotic, possibly temporal, conditions such as interstellar shock waves (Field *et al.* 1968) must be introduced to raise temperatures so that reaction rates proceed faster than photodissociation. This is particularly true if $OH/H = 10^{-4}$ as Robinson, Gardner, van Damme, and Bolton (1964) have found in one case, or even if $OH/H = 10^{-8}$ to 10^{-7} as Goss (1967) often finds.

It appears possible to confirm the physical picture presented here by performing an OH emission survey of many dust clouds to obtain information on the existing ranges of relative OH abundance. Also, attempts to correlate 21-cm emission with dust, as performed by Garzoli and Varsavsky (1966) and P. Mészáros and C. Varsavsky (private communication) are valuable, because we expect OH emission only in those objects which have much H_2 if the production process is reaction (9); detailed presentation of complete 21-cm line data is helpful, however (cf. cloud 1F). Limits on the OH spin temperature can be determined, and if accurate enough data is available the actual spin temperature can be found. Further confirmation also demands more accurate estimates of the total extinction in the clouds; photodissociation rates are extremely sensitive to the extinction and the crude estimates presented here are hardly adequate. Of course, more information on reaction rates and consideration of other possible reactions are necessary, and special attention must be given to more efficient production mechanisms at low temperatures such as tunneling.

The exciting possibility of mapping motions within the complex dust clouds we see on optical photographs is now available. Further observations of OH emission in dust clouds are presently being undertaken by the author.

The very existence of this paper depends on the excellent technical facilities and personnel provided by the Radio Astronomy Laboratory at Berkeley and its Hat Creek Observatory. Fruitful discussions with Drs. B. Turner, P. Aannestad, G. Field, W. W. Goss, W. D. Gwinn, and H. Weaver contributed much to this paper, and Drs. N. H. Dieter, B. Turner, and an anonymous referee kindly read the manuscript and suggested several important improvements. A serious error in OH production rate was pointed out by Dr. P. Solomon. This work was supported in part by NSF grant GP-7729.

Note added in proof: Mr. P. Mészáros kindly pointed out to the author Bok's (1956) star counts in the dark clouds in Taurus and Ophiuchus, the same ones studied here. Bok derives lower limits for extinction of 6.7 mag and 7–8 mag, respectively, for the centers of these clouds. Our crude estimates, then, are not inconsistent with his more precise work.

REFERENCES

Allen, C. W. 1963, *Astrophysical Quantities* (London: Athlone Press).
Bok, B. 1937, *The Distribution of Stars in Space* (Chicago: University of Chicago Press).
———. 1956, *A.J.*, **61**, 309.
Carroll, T. D., and Salpeter, E. E. 1966, *Ap. J.*, **143**, 609.
Dunham, T. Jr. 1938, *Proc. Am. Phil. Soc.*, **81**, 277.
Field, G. B., Rather, J. D. G., Aannestad, P. A., and Orszag, S. A. 1968, *Ap. J.*, **151**, 953.
Garzoli, S. L., and Varsavsky, C. 1966, *Ap. J.*, **145**, 79.
Goss, M. 1967, *Ap. J. Suppl.*, No. 137.
Gould, R. J., and Salpeter, E. E. 1963, *Ap. J.*, **138**, 393.
Heiles, C. 1966, *A Catalog of Hydrogen-Line Data at Intermediate Galactic Latitudes* (National Radio Astronomy Observatory, Green Bank, West Virginia).
———. 1967*a*, *Ap. J.*, **148**, 299.
———. 1967*b*, *Ap. J.*, *Suppl.*, No. 136.
———. 1967*c*, *A J.*, **72**, 1040.
Hoffleit, D. 1964, *Yale Catalogue of Bright Stars* (New Haven, Conn.: Yale University Observatory).
Hubble, E. 1934, *Ap. J.*, **79**, 8.
Hulst, H. C. van de. 1949, *Recherches Astr. de l'Obs. Utrecht*, **11**, part 2.

Hulst, H. C. van de, Muller, C. A., and Oort, J. H. 1954, *B.A.N.*, **12**, 117.
Keenan, P. C. 1963, in *Basic Astronomical Data*, ed. K. Aa. Strand (Chicago: University of Chicago Press), p. 78.
Knapp, H. F. P., Meijdenberg, C. J. N. van den, Beenakker, J. J. M., and Hulst, H. C. van de. 1966, *B.A.N.*, **18**, 256.
Lilley, A. E. 1955, *Ap. J.*, **121**, 559.
Lynds, B. T. 1962, *Ap. J. Suppl.*, **7**, 1.
McCuskey, S. W. 1941, *Ap. J.*, **94**, 468.
Miller, F. D. 1938, *Harvard Ann.*, No. 105, p. 297.
Müller, R. 1931, *Zs. f. Ap.*, **3**, 369.
Palmer, P., and Zuckerman, B. 1967, *Ap. J.*, **148**, 727.
Rhijn, P. J. van. 1929, *Pub. Kapetyn Astr. Lab.*, No. 43.
Robinson, B. J , Gardner, F. F., Damme, K. J. van, and Bolton, J. G. 1964, *Nature*, **202**, 989.
Slocum, L. T., and Sitterly, B. W. 1937, *Harvard Bull.*, No. 905, 16.
Solomon, P., 1968, *Ap. J.* (in press).
Stecher, T. P., and Williams, D. A. 1966, *Ap. J.*, **146**, 88.
———. 1967, *Ap. J.*(Letters), **149**, L29.
Swamy, K. S. Krishna, and O'Dell, C. R. 1967, *Ap. J.*, **147**, 937.
Turner, B. E. 1966, *Nature*, **212**, 184.
Weaver, H. F. Dieter, N. H., and Williams, D. R. W. 1968, *Ap. J. Suppl.*, in press.
Whipple, F. 1946, *Ap. J.*, **104**, 1.
Wickramasinghe, N. C. 1965, *M.N.R.A.S.*, **131**, 177.